-Technical Paper-

SHEAR PERFORMANCE OF R/C FOUNDATION BEAM USING 785 CLASS SHEAR REINFORCEMENT WITH HOOKED LAP SPLICING

Nikesh MAHARJAN[*1], Makoto MARUTA[*2], Masato OGATA[*3]

ABSTRACT

The use of lap splice in shear reinforcement, as recommended in *AIJ Recommendation for Detailing and Placing of Concrete Reinforcement* is limited to SD490 and below. Hence, to study its applicability on higher strength rebars, the authors conducted cantilever RC foundation beam tests using 785N/mm^2 weld-spliced and lap-spliced shear reinforcement. The strength characteristics exhibited by lap-spliced specimens were comparable to weld-spliced specimens, and they were safe at allowable loads calculated as per AIJ Guideline, as well as ultimate loads, calculated using Arakawa Mean and Modified Plasticity Equations.

Keywords: High Strength Rebar, Lap Splice, Allowable Shear Strength, RC Foundation Beam

1. INTRODUCTION

The depth of an RC foundation beam may range up to 4-5m in high-rise buildings. These deep beams with lower shear span ratio have a greater shear demand. Recently, high strength shear rebars (685N/mm^2 and above) are being commonly used to reduce the amount of shear rebar required. However, constructing shear reinforcement using welded joints or with hooks at end are quite difficult in foundation beams due to their large size. Therefore, it is desirable to provide lap splicing at about middle height of the beam depth, reducing the length of the rebar in the direction parallel to the beam depth, thus easing construction process.

According to RC Reinforcement Detailing Guideline [1], lap splicing of length L_{1h} with a hook can be provided in the middle portion of foundation beams in case of rebar SD490 and below. However, this lap length is believed to be specified based on the necessity of construction and engineering judgment, rather than on the outcome of an experiment [2]. On one hand, the use of high-strength rebar (685N/mm^2 and 785N/mm^2) is beyond the scope of the current guideline. On the other hand, the shape and size of ribs and knots of high-strength rebar available in the market currently differ from those of regular deformed bars, such as SD490 and below. As a result, the suitability of the guideline for use with high strength rebars is unknown. Hence, an experimental study on the performance of foundation beam using shear reinforced bar with a hooked lap splice is necessary.

In this study, cantilever foundation beam tests were conducted to determine the shear performance of foundation beams with lap-spliced shear rebar (hereafter, lap-spliced specimen) and compared with foundation beam with weld-spliced rebar (hereafter, weld-spliced specimen) in terms of maximum shear strength exhibited, progression of shear cracks, and strain with the increase in the rotation angle of the specimen. The shear performance of the specimens was then evaluated using calculated design values of allowable shear strength as per Standard for Structural Calculation of Reinforced Concrete Structures, 2018 [3] (hereafter, AIJ Guideline) and ultimate shear strength according to Arakawa Mean Equation and Modified Plasticity Equation [4].

2. EXPERIMENTAL PROGRAM

2.1. Description of Test Specimen

As illustrated in the Table 1 and Fig. 1, the experiment uses four specimens. The test object consists of a rigid stub in the middle and cantilever foundation beam specimens on its either side. The left and right parts consist of weld-spliced specimen and lap-spliced specimen, respectively. The lap splices are provided with 135° hooks at the end. The foundation beam specimens are each of size 250 x 800mm and have the shear span ratio 1.55. Each specimen consists of longitudinal reinforcement of 3+3-D25 (SD490) at top and bottom.

Table 1. Specimen Outline

Specimen	Fc (N/mm^2)	Shear Reinforcement	
		Pw (%)	Lap Length
FG-21-W	21	0.23	−
FG-21-45	21	0.23	45d
FG-30-W	30	0.23	−
FG-30-40	30	0.23	40d

Fc : Characteristic Compressive Strength of Concrete
d : Nominal Diameter of Reinforcement Bar
Pw : Shear Reinforcement Percentage

*1 Graduate Student, Dept. of Architecture, Shizuoka Institute of Science and Technology, JCI Student Member
*2 Professor, Dr. of Eng., Shizuoka Institute of Science and Technology, JCI Fellow Member
*3 Engineer, Research and Development Section, Tokyo Tekko Co., Ltd.

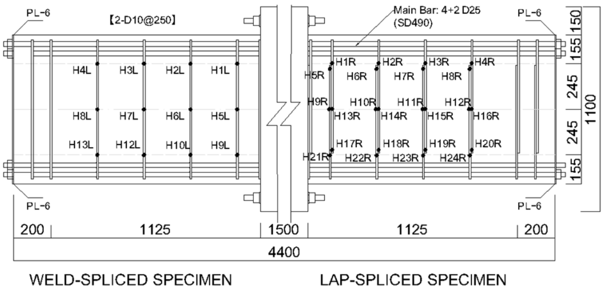

(a) Reinforcement Details & Strain Measurement Points of Foundation Beam Specimens

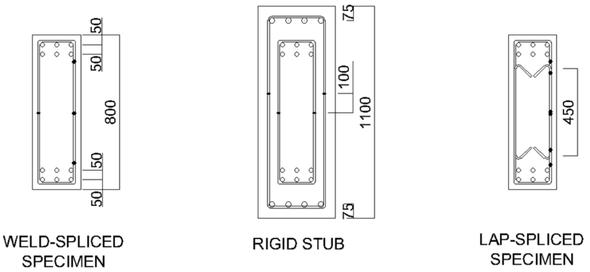

(b) Cross Section of Foundation Beam Specimens

Fig. 1 Foundation Beam Specimen

2.2 Material Properties

The compressive strength of concrete for each specimen was determined from the average of three test specimens. The 28-day average strength was 19.8N/mm^2 and 30.1N/mm^2 for specimens with compressive strength of 21N/mm^2 and 30N/mm^2, respectively. The average tensile yield strength of three test samples of longitudinal reinforcement of foundation beams and stub, obtained from tensile tests, was 536N/mm^2. Similarly, the yield strength of shear reinforcement was 852N/mm^2. Other materials properties derived from material testing are shown in Table 2.

Table 2. Material Data and Results

(a) Reinforcement Bar

Rebar Type	Rebar Name	Applied Position	σ_y (N/mm^2)	ε_y (μ)	σ_u (N/mm^2)	Elongation (%)
SD490	D25	Main Bar (Beam)	536	3175	701	22
SD490	D29	Main Bar (Stub)	536	3051	719	23
SD785	T10	Shear Reinforcement	852	4322	1018	15

σ_y : Yield Strength ε_y : Yield Strain

σ_u : Ultimate Tensile Strength

Es : Young's Modulus of Elasticity of Steel

(b) Concrete

Fc (N/mm^2)	Specimen	σ_B (N/mm^2)	ε_c (μ)	E_c (N/mm^2)
21	FG-21-W	19.8	1666	26200
	FG-21-45			
30	FG-30-W	30.1	2204	26500
	FG-30-40			

Fc : Characteristic Compressive Strength of Concrete

σ_B : Averaged Experimental Value of Concrete Strength

ε_c : Strain at Strength σB

E_c : Young's Modulus of Elasticity of Steel

u : Poisson's Ratio

2.3 Experimental Procedure

The experiment was conducted on a stiff steel frame, as shown in Fig. 2. Load was applied on the ends of each specimen, alternately from top and bottom, using hydraulic jacks. The specimens were rotated until the Damage Control Short-term Allowable Load, Q_{AS} (Ref. section 4.1) was reached in the first cycle and the loading was then repeated for the second cycle. Next, the specimens were rotated until the Safety Level Short-term Allowable Load, Q_A (Ref. section 4.1) was reached. After that, the specimens were rotated at R= 2.5, 5.0 x 10^{-3} rad., for two cycles each. Loading of FG-21-W and FG-21-45 were stopped after rotation angle of 10 x 10^{-3} rad. due to excessive crushing and spalling of concrete. FG-30-W and FG-30-40 were rotated to 20 x 10^{-3}rad. The loading sequence is shown in Fig. 3.

The crack widths were measured at peak loads, Short-term Allowable Load, Long-term Allowable Load and unloaded condition at different cycles as shown in Fig. 3, using crack width ruler.

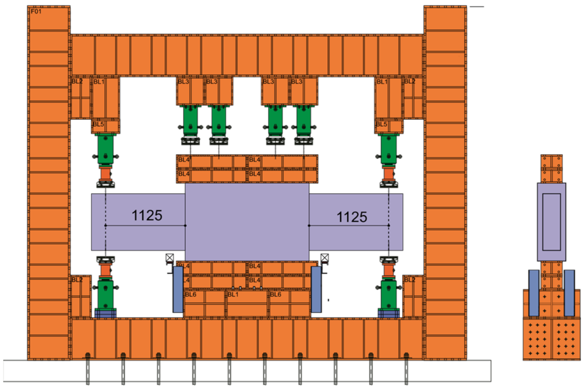

Fig. 2 Frame and Test Specimen

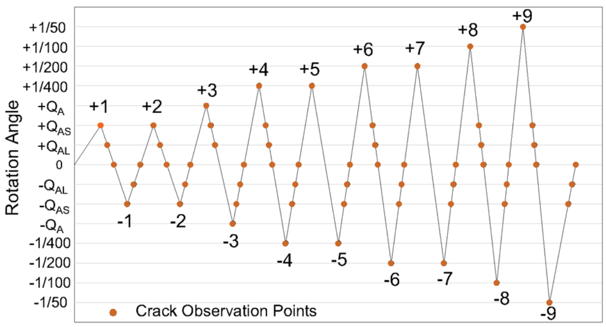

Fig. 3 Rotation History

3. RESULTS AND DISCUSSION

3.1 Load – Deformation relation of each specimen and failure condition

Fig. 4 shows the Load-Rotation curves for each specimen. The figure also indicates the occurrence of the first flexural crack, first shear crack, and maximum load carrying capacity (Q_{max}) exhibited by the specimen. Additionally, the figure shows the datum line

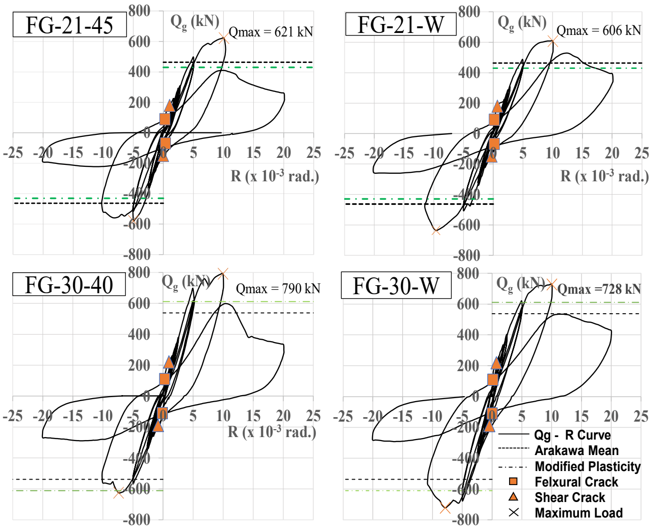

Fig. 4 Load-Rotation Curve

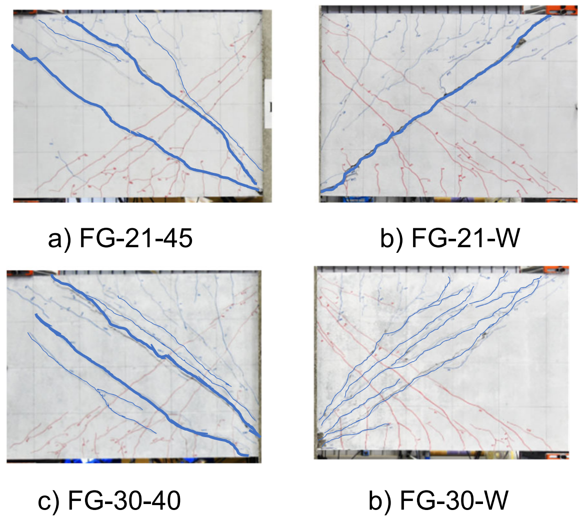

Fig. 5 Shear Cracks in the Specimens at Failure

representing calculated values of ultimate shear strength according to Arakawa Mean and Modified Plasticity equations.

Irrespective of the splice type and characteristic compressive strength of the concrete, all specimens showed maximum shear strength at a rotation angle of approximately 10 x 10^{-3}rad. Once the maximum shear strength was surpassed, the crack width increased rapidly at the flexural compression zone near the end of the specimen (Fig. 5). It is to be noted that none of the specimens experienced flexural yielding of the main bars, as per the design.

Fig. 5 shows the crack conditions during maximum strength (10×10^{-3} rad. positive cycle). In the weld-spliced specimen, shear cracks tend to concentrate along the diagonal direction. However, in lap-spliced there are significantly fewer cracks in the diagonal portion. Two major shear cracks were visible in lap-spliced specimen, with other minor cracks occurring on the outer side of those major cracks. The fewer number of cracks along the diagonal region in the lap-spliced specimen is likely due to presence of two rebars acting together to resist the load. However, this tendency was not observed in subsequent negative loading due reduction of bond between shear rebar and concrete.

3.2 Shear force ratio Q/Q_{fu} - rotation angle R relation

Fig. 6 shows the envelope curve of the Q/Q_{fu} - R relation, where Q/Q_{fu} represents the ratio of experimental shear strength of the specimen to the calculated shear force at the time of ultimate flexural strength. The Q_{su}/Q_{fu} datum line is also depicted in the same figure, which represents the ratio of shear force calculated using Arakawa Mean Equation and ultimate flexural strength of the beam. Based on the curves, the following observations were made.

(1) The maximum shear strengths exhibited by all the specimens exceeded the values calculated by Arakawa Mean equation for the ultimate shear strength of an RC beam. The rotation angle at maximum strength at both positive and negative

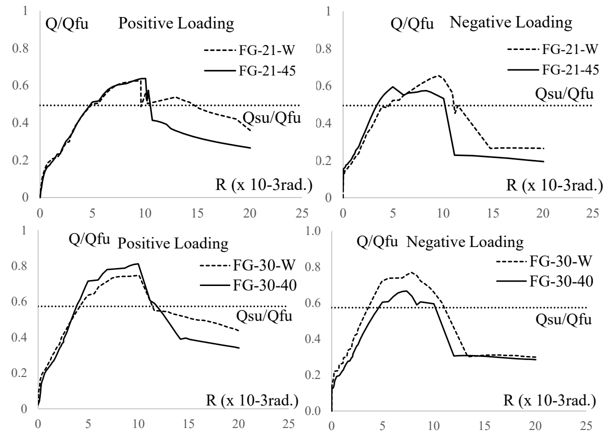

Fig. 6 Envelope Curve of Q/Q_{fu} vs R

loading cycles was about 10×10^{-3}rad. in all cases.

(2) The lap-spliced specimens showed slightly higher maximum strength than weld-spliced specimens at positive cycle, possibly due to two shear rebars at lap joint. However, at negative cycle, lap-spliced specimens had a lower maximum shear strength due to reduced bonding action after pull-out of hooks at the end of lapping (Ref. section 3.4), that occurred at the preceding positive cycle.

(3) The reduction of shear strength commenced after surpassing rotation angle 10×10^{-3}rad. in all specimens. The decrease of strength was slightly more rapid in the lap-spliced specimens after reduction is shear strength due to pull-out of shear rebars at lapping portion.

3.3 Progression of Shear Cracks

The shear cracks were initiated at a rotation angle of $0.6\text{-}1.0\times10^{-3}$rad. and increased steadily with each load cycle. Fig. 7(a) shows that the progress of maximum shear crack width was similar in both weld-spliced specimens and lap-spliced specimens. This suggests that the type of splice used (weld-splice or lap-splice) had little effect on the crack width progression. Both specimens of Fc 30N/mm^2, showed a decrease in crack width after a rotation angle of 10×10^{-3} rad. due to concrete crushing. Similarly, both specimens of Fc 21N/mm^2 experienced more concrete crushing and spalling beyond the same rotation angle (10x10^{-3} rad.) due to weaker concrete strength.

The Fig. 7(b) shows the progression of maximum residual shear cracks width under unloaded condition with respect to the increase in rotation angle. In general, the residual crack width of specimens with compressive strength of 21N/mm^2 was observed to increase more rapidly after a rotation angle 5x10^{-3}rad. compared to specimens with the compressive strength of 30N/mm^2. According to the AIJ Guideline, residual crack values for RC structures are limited to 0.2mm-0.25mm for the inner surface and 0.3-0.4mm for the outer surface [3]. In this study, a limiting value of 0.3mm was selected for residual shear crack. The residual cracks after surpassing the rotation (R_{AS3}) at Damage Control Short-Term Allowable Load (Q_{AS3}) was found to be below 0.3mm in all the specimens.

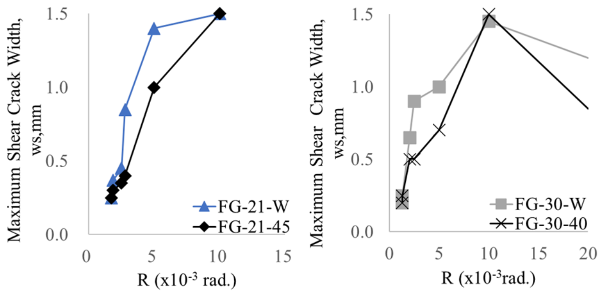

(a) Maximum Shear Crack Width at Peak Load at Each Cycle

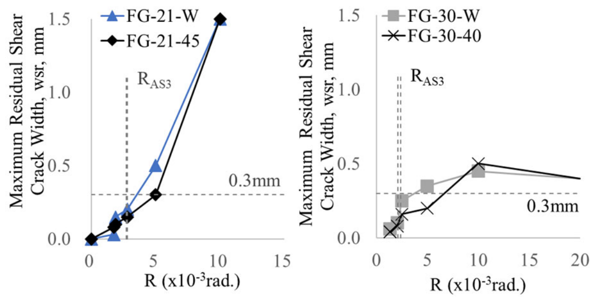

(b) Maximum Residual Shear Crack Width at Each Cycle

Fig. 7 Progression of Maximum Shear Crack Width

3.4 Shear Strain on Reinforcement Bar

The strain progression on the mid-portion of shear reinforcement for each specimen is shown in Fig. 8. Generally, the maximum strain occurs in the 2nd and 3rd shear reinforcements from the stub, which correspond to the wider crack widths in that region (Fig. 5). Fig. 9 illustrates a comparison of the maximum strain at top, middle and bottom portions of the shear rebars in the welded and lap-spliced specimens. The key observations are as follows:

(1) All specimens showed a rapid increase in strain after a rotation angle of 5x10^{-3}rad., with weld-spliced specimens experiencing a more significant increase and surpassing yield strength before reaching the rotation angle of 10x10^{-3}rad. Lap-spliced specimens

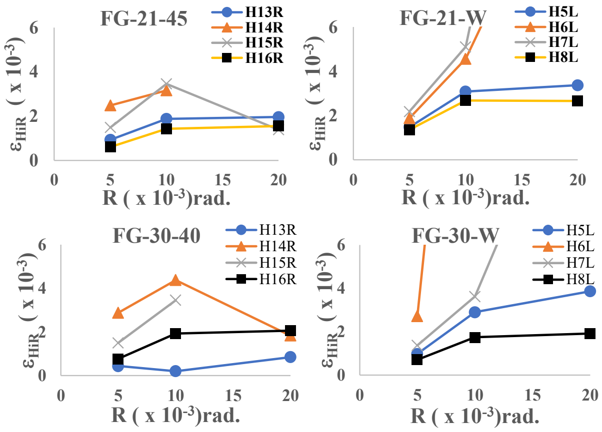

Fig. 8 Comparison of Strain in Each Shear Reinforcement at Mid-portion

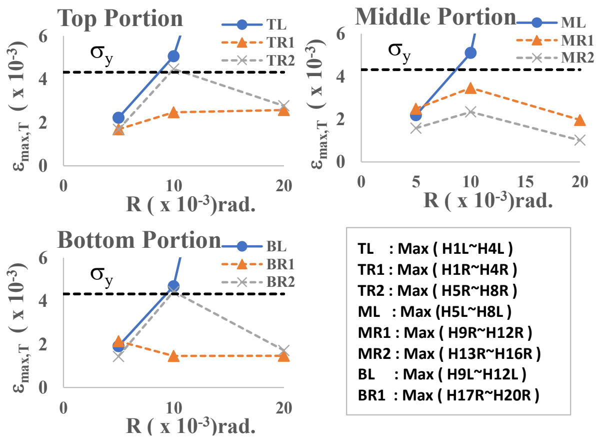

(a) Specimens FG-21-W and FG-21-45

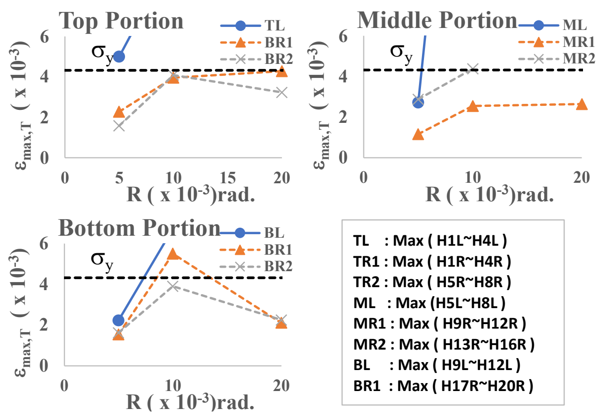

(b) Specimens FG-30-W and FG-30-40

Fig.9 Maximum Strain at Shear Reinforcement

had lower strains likely due to presence of two shear rebars at lapping portions.

(2) Although the lap-spliced shear reinforcement did not yield in both specimens and had lower strain overall, the crack width progression was similar to that of weld-spliced specimens (Fig. 7). This indicates that, in addition to tensile strain in shear reinforcement, the relative displacement (pull out) of shear reinforcement at lapped portion also contributes to the crack widening. The residual cracks observed in the unloaded lap-spliced specimens also suggest the occurrence of pull-out.

4. CONFIRMATION OF TARGET PERFORMANCE LEVEL

4.1 Long-Term and Short-Term Allowable Load

The shear performance of test specimens was evaluated using long-term and short-term allowable shear force as defined in AIJ Guideline.

(1) Serviceability level Long-Term Allowable Load

The considerations for ensuring serviceability against shear forces under long-term loading are as follows:

(a) $Q_{AL1} = b.\,j.\,\alpha.\,f_s$ (without cracks) (1)

(b) $Q_{AL2} = b.\,j.\,\{\alpha.f_s + 0.5\,{}_wf_t.\,(p_w - 0.002)\}$ (2)

Eq. 2 is used for evaluating Long-term load when formation of shear cracks are allowed. The calculated Q_{AL1}, Q_{AL2} values are compared to the experimental value of shear force at the time of crack formation. Table. 3 shows that the shear forces at the time of crack formation ${}_sQ_{cr}$ is greater than Q_{AL1} and Q_{AL2}.

(2) Damage Control Level Short Term Allowable Load

The considerations for damage control against shear forces due to short term loading is as follows:

(a) $Q_{AS} = b.\,j.\,\{\beta_c.\alpha.f_s + 0.5\,{}_wf_t.\,(p_w - 0.002)\}$ (3)

where,

b : Beam Width

j : Lever Arm

fs : Short-Term Allowable Shear Stress of Concrete

${}_wf_t$: Short Term Allowable Shear Stress of Shear Reinforcement Bar, ${}_wf_t$=590 N/mm^2

p_w : Shear Reinforcement Ratio

β_c : Correction Coefficient Related to p_w = 2/3

α : Coefficient Related to Span Ratio (M/Q_d)

In AIJ Guideline, the value of β_c is mentioned to be 2/3. But, in case of beam with lower value of shear reinforcement ratio, p_w, shear cracks do not occur of the calculated Q_{AS} value, resulting in the under evaluation of actual short-term load. Table 3. shows that such was the case, in present study. The shear force, ${}_sQ_{cr}$ at which cracks were formed, was greater than Q_{AS1}. Hence, Eq. 3 was modified into three cases varying the value of βc (2/3~1), based upon the work of Ichioka et al. [5] as follows:

CASE I (Q_{AS1}) : βc = 2/3, (p_w-0.002)

CASE II (Q_{AS2}) : βc = Eq. (4), (p_w-0.002)

CASE III(Q_{AS3}) : βc = Eq. (4), (p_w-0.001)

The term (p_w-0.001) is used in CASE III to account for the increase in shear strength due to the use of high strength shear reinforcement bar. The value of βc linearly varies from 2/3 at p_w=1.2% to 1 at p_w=0.2%.

$\beta c = 1 - (100p_w - 0.2)/3$ (4)

(3) Safety Level Short-Term Allowable Load

The considerations for ensuring safety against loads during strong earthquake motion, Q_A according to AIJ Guideline was modified into two cases as:

(a) $Q_{A1} = b.\,j.\{\,\alpha.f_s + 0.5\,{}_wf_t.(p_w - 0.002)\}$ (5)

(b) $Q_{A2} = b.\,j.\,\{\,\alpha.f_s + 0.5\,{}_wf_t.\,(p_w - 0.001)\}$ (6)

The calculated values of the allowable shear strength for above mentioned Performance levels and their respective rotation angles are shown in Table. 3.

4.2 Comparison of Short-Term Allowable Shear Force and Maximum Shear Strength:

The Q_{max}/Q_{fu} - Q_{ASi}/Q_{fu} relation is shown in Fig. 11. The figure also includes previous data on similar foundation beam test with 685 N/mm^2 rebars performed by Masao [2]. It is to be noted that in contrast to the specimen used in the study, the specimens in current experiment are designed such that main rebars do not yield, i.e., specimen undergo shear failure and crushing of concrete before reaching maximum flexure strength, resulting smaller value of the Q_{max}/Q_{fu} ratio.

The figure shows that all specimens whether weld-spliced or lap-spliced, the shear strengths are safe at Damage Control Short-term Allowable Load. Similarly, Q_{max}/Q_{fu}-Q_{Ai}/Q_{fu} relation is shown in Fig. 12. The figure shows that regardless of the splice type, the shear strengths of the specimens are on the safe side at the Safety Level Short-term Allowable Load.

4.3 Comparison with Calculated Ultimate Shear Strength

The maximum shear strength of each specimen was compared using Arakawa Mean Equation (Q_{suA}) and Modified Plasticity Equation (Q_{suP}) calculated as follows:

(a) Arakawa Mean Equation

$$Q_{suA} = \left[0.068.\,p_t^{0.23}.\frac{Fc+18}{\frac{M}{Q.d}+0.12} + 0.85\sqrt{p_w.\,\sigma_{wy}}\right] b.j \quad (7)$$

(b) Modified Plasticity Equation

$Q_{suP} = b.j.p_w.\sigma_{wy}. + k_1 + (1-k_2).b.\,D.\,\nu.\,Fc$ (8)

where,

Fc : Compressive Strength of Concrete

p_t : Percentage of Longitudinal Reinforcement

σ_{wy} : Yield Strength of Shear Reinforcement

Table:3 Long and Short-Term Allowable Shear Strength of Each Specimen

Specimen		Long Term Allowable Load				Damage Control Short Term Allowable Load						Safety Level Short Term Allowable Load			
		Case I		Case II		CASE I βc =2/3 (pw-0.002)		CASE II βc =1-(100pw-0.2)/3 (pw-0.002)		CASE III βc =1-(100pw-0.2)/3 (pw-0.001)		CASE I (pw-0.002)		CASE II (pw-0.001)	
	sQcr	QAL1	RAL1	QAL2	RAL2	QAS1	RAS1	QAS2	RAS2	QAS3	RAS3	QA1	RA1	QA2	RA2
FG-21-W	180	164	0.6	168	0.6	177	0.7	257	2.2	304	2.8	259	2.2	306	2.8
FG-21-45	180	164	0.8	168	0.9	177	1.0	257	2.1	304	2.7	259	2.2	306	2.7
FG-30-W	220	197	0.5	201	0.5	210	0.6	305	1.6	352	2.1	308	1.6	355	2.1
FG-30-40	220	197	0.7	201	0.7	210	0.8	305	1.9	352	2.4	308	2.0	355	2.4

$$k_1 = \left[\sqrt{(L/D)^2+1} - (L/D)\right]/2 \quad (9)$$

$$k_2 = 2.p_w.\sigma_{wy}/(\nu.Fc) \quad (10)$$

$$\nu = 0.7.\ (0.7\text{-}Fc/200) \quad (11)$$

Fig. 13(a) and 13(b) shows Q_{max}/Q_{fu} - Q_{suA}/Q_{fu} and Q_{max}/Q_{fu} - Q_{suP} /Q_{fu} relations, respectively. The observations from the figures are:

(1) The shear strengths exhibited by all the specimens in the experiments were on the safer sider when evaluated with the ultimate shear force values calculated by Arakawa Mean and Modified Plasticity equations.

(2) There wasn't any significant difference in the Q_{max}/Q_{fu} - Q_{su} /Q_{fu} relation between specimen using weld-spliced and lap-spliced specimen.

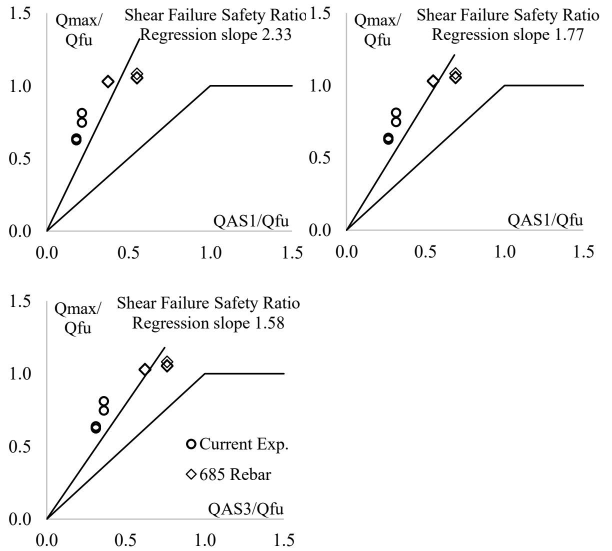

Fig. 10. Q_{max}/Q_{fu} – Q_{ASi}/Q_{fu} (Damage Control Level)

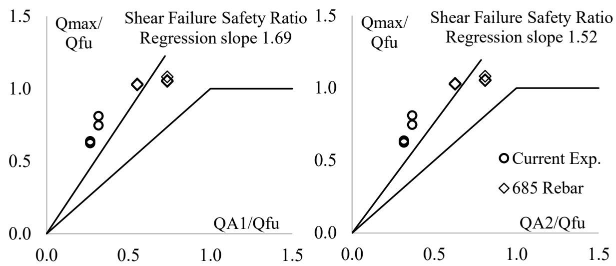

Fig.11. Q_{max}/Q_{fu} – Q_{Ai}/Q_{fu} (Safety Level)

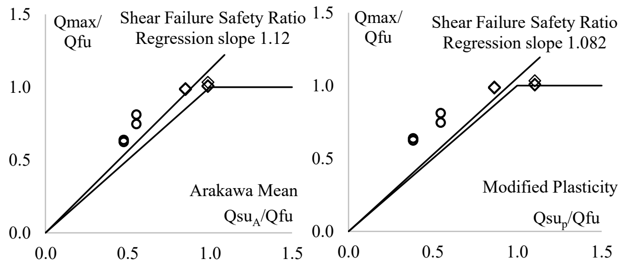

(a) Arakawa Mean (b) Modified Plasticity

Fig. 12. The Q_{max}/Q_{fu}-Q_{su}/Q_{fu} Relation

5. CONCLUSIONS

The main conclusions from this study are summarized as follows:

(1) The lap-spliced foundation beam specimens showed a slightly higher maximum shear strength than the weld-spliced specimens at the positive cycle, likely due to two shear rebars working together to resist the load. On the contrary, the lap-spliced specimens had a lower maximum shear strength at negative cycle due to a reduction in the bonding action between the rebar and concrete. However, in general, there was no significant difference between the maximum strength exhibited and load-rotation relation between lap-spliced and weld-spliced foundation beam.

(2) Both the maximum shear crack and maximum residual shear crack exhibited similar progression in both weld-spliced and lap-spliced specimens. The residual crack in weld-spliced specimen was due to yielding of shear rebars, while in lap-spliced specimens, it was caused by pull-out of shear rebars at lapping portion.

(3) The lap-spliced foundation beam specimens were safe at various levels of allowable loads calculated as per AIJ Guideline and the ultimate loads calculated using Arakawa Mean and Modified Plasticity Equations.

ACKNOWLEDGEMENT

The authors wish to thank Mr. Satoru Nagai of S.K. Services for his invaluable assistance in the experimental program and our fellow undergraduate student Mr. Naruya Ohira for his assistance throughout the study.

REFERENCES

[1] Architectural Institute of Japan, "Recommendation for Detailing and Placing of Concrete Reinforcement," (In Japanese), 2010.

[2] K. Masao, "Shear Behavior of R/C Footing Beams with Hook Lap Splices Using 785 and 685 Class Shear Reinforcements," Summaries of Technical Papers of Annual Meeting, Vol. IV, pp.455-456 (In Japanese), Architectural Institute of Japan, September, (In Japanese), 2015.

[3] Architectural Institute of Japan, "AIJ Standard for Structural Calculation of Reinforced Concrete Structures," (In Japanese), 2018.

[4] Architectural Institute of Japan, "Design Guidelines for Earthquake Resistant Reinforced Concrete Buildings Based on Ultimate Strength Concept," (In Japanese), 1990

[5] Y. Ichioka, H. Tagawa, M. Adachi, and K Masuo, "Allowable Shear Strength Controlled by Residual Shear Crack Width of R/C Beams Using SD295 to 785N/mm² Shear Reinforcement," J. Struct. Constr. Eng., AIJ, Vol. 76 No.662, 821-828, (In Japanese), Apr. 2011